JACS
JOURNAL OF THE AMERICAN CHEMICAL SOCIETY
Cite This: J. Am. Chem. Soc. 2018, 140, 10644−10648
Communication
pubs.acs.org/JACS

Enantioselective Synthesis of α-Amidoboronates Catalyzed by Planar-Chiral NHC-Cu(I) Complexes

C. Benjamin Schwamb,[†] Keegan P. Fitzpatrick,[†] Alexander C. Brueckner,[‡] H. Camille Richardson,[‡] Paul H.-Y. Cheong,[‡] and Karl A. Scheidt*[,†]

[†]Department of Chemistry, Center for Molecular Innovation and Drug Discovery, Northwestern University, Silverman Hall, Evanston, Illinois 60208, United States

[‡]Department of Chemistry, Oregon State University, 153 Gilbert Hall, Corvallis, Oregon 97331, United States

Supporting Information

ABSTRACT: The first highly selective catalytic hydroboration of alkyl-substituted aldimines to provide medicinally relevant α-amidoboronates is disclosed. The Cu(I)-catalyzed borylation proceeds with excellent facial selectivity when a set of planar-chiral N-heterocyclic carbenes (NHCs) were employed as ligands. Density functional theory computations suggest that interactions between BPin and the planar-chiral catalyst are responsible for the observed stereoselectivity. Important pharmacophores, such as the boronate analogue of isoleucine, can be prepared using a chromatography-free protocol starting from commercially available reagents. The application of these NHC ligands in these Cu(I)-catalyzed processes offers a significant contribution to existing strategies for laboratory-scale preparation of enantioenriched α-amidoboronates.

Boronic acids are widely useful reagents in organic synthesis and constitute an important class of medicinal pharmacophores.[1] Since the discovery of the inhibitory properties of boronic acids against serine proteases,[2] α-amidoboronic acids have emerged as particularly useful for selective proteosome inhibition.[3] Consequently, the α-amidoboronate moiety can be used as an electrophilic "warhead" for covalent protease inhibition, guided by the peptide to which it is attached.[3c,e,4] The approval of Velcade (Figure 1) in 2003 was a breakthrough clinical application of a boronic acid peptidomimetic,[5] and since then, a rise in the number of therapeutics using the α-amidoboronate motif has been accompanied by increasing efforts toward their efficient synthesis.[6] The majority of therapeutically relevant α-amidoboronates bear an α-alkyl functionality,[7] yet surprisingly there are limited means to access these compounds in a catalytic enantioselective manner.[8] In 1980, Matteson reported the homologation of a chiral pinanediol to yield an α-chloroboronic ester and subsequent nucleophilic displacement to yield the α-amino adduct.[9] Alternatively, the diastereoselective borylation of *N*-*tert*-butylsulfinyl aldimines by Ellman avoids the use of organolithium reagents and is diastereoselective in nature (Figure 1).[10] Very recently, Baran has reported a decarboxylative approach to install boronic acids that can accommodate α-amino acid substrates.[11] In addition to their therapeutic potential, α-amidoboronates could serve as potential metal-catalyzed cross-coupling partners, if both aryl- and alkyl-substitutued species could be accessed with high levels of efficiency and selectivity.

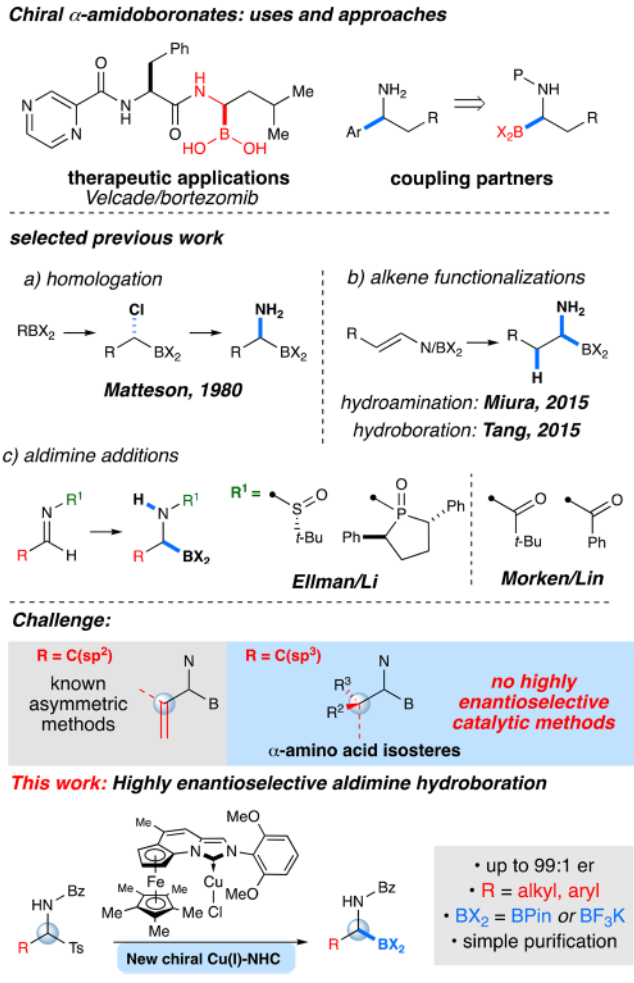

Figure 1. Overview of α-amidoboronate synthesis strategies.

While enantioselective imine borylations to access alkyl amidoboronates currently operate at levels below synthetic utility, some alternative approaches to construct this motif via

Received: May 14, 2018
Published: August 13, 2018

DOI: 10.1021/jacs.8b05045
J. Am. Chem. Soc. 2018, 140, 10644−10648

alkene functionalization have recently emerged.[12] For example, Miura disclosed an elegant Cu(I)-catalyzed hydroamination of alkenyl boronates to produce tertiary amines,[12a] while Tang accessed enantioenriched tertiary aminoboronates via a Rh(I)-catalyzed hydroboration.[12b] Given the increasing utility of α-alkyl amidoboronates and the dearth of processes to produce them enantioselectively, we sought to develop a system that could (1) deliver α-alkylamidoboronates directly from imines, (2) use starting materials readily prepared from commercially available reagents, and (3) leverage the unique steric and topological characteristics of our family of planar chiral N-heterocyclic carbene ligands.

We have been engaged in developing Lewis bases for organocatalysis and transition-metal-mediated processes,[13] with a focus on new classes of N-heterocyclic carbenes (NHCs). We disclosed the development of a distinct class of planar-chiral NHCs in 2015,[14] which are based on the pyridine-annulated iron sandwich complexes pioneered by Fu.[15] These ferrocene-based imidazolium derivatives possess tunable elements, allowing for a variety of substituents to be introduced on either the iron-complexed N-heterocyclic scaffold and/or the lower cyclopentadienyl (Cp) ring. We anticipated that the atypical stereochemical environment presented by these NHCs as ligands could be exploited to enable asymmetric organometallic transformations that remain unsolved using the current state of the art. To enhance our limited understanding of the relevant molecular and structural interactions present in this otherwise unexplored class of NHCs, we anticipated that modeling studies (empirical and *in silico*) would be crucial to benchmark the reactivity and selectivity of these NHCs as ligands for asymmetric organometallic catalysis.

A survey of asymmetric transformations facilitated by chiral Cu(I)-NHC complexes identified that the asymmetric diboration of *alkyl* aldimines remains a significant gap in the knowledge to date. We initiated our studies on this reaction first with respect to identifying compatible imine substrates for our catalysts. A preliminary reaction screen using Cu(I)-NHC catalyst **A**, B_2Pin_2, and 10 mol % NaO*t*-Bu in toluene revealed *N*-benzoyl-protected α-tosylamines (e.g., **1a**, Figure 2A) as ideal imine precursors. *N*-Benzoyl cyclohexylimine generated *in situ* via deprotonation of **1a** with excess Cs_2CO_3[8c] gave adequate yields of the desired α-amidoboronate **2a** (Figure 2A, entry 2). Further evaluation identified catalyst **C** as capable of facilitating the reaction with high enantioselectivity (97:3 er). Surprisingly, catalysts bearing larger substitution on the wingtip *N*-aryl ring or the Cp ring of the ferrocene decreased both enantiomeric ratio (er) and yield (entries 1–7). In the absence of CuCl, no significant conversion was observed using the precursor imidazolium chloride to **C**, thus discounting a metal-free mechanism.[10c] In contrast to the analogous hydroboration of alkenes,[16] we found that protic additives completely suppressed the reaction (entry 11). Other alkoxide bases led to decreased er in all cases (entries 12–14). Switching from Cs_2CO_3 to K_2CO_3 negatively impacted yield, presumably due to slower aldimine formation; however er remained unaffected (entry 16).

We were intrigued by the wide variability in reaction enantioselectivity among the different Cu(I)-NHC catalysts screened. For instance, pentaphenyl-Cp-derived catalysts **B**, **D**, and **G** all gave product with uniformly low yield (~40%) and modest er (~70:30). To gain a better sense of the steric demand presented by these ligands in comparison to other

A. Reaction optimization

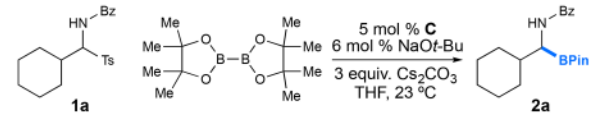

entry	modification	yield (%)[b]	er[c]
1	none	91	97:3
2	**A** instead of **C**	78	69:31
3	**B** instead of **C**	42	71:29
4	**D** instead of **C**	36	68:32
5	**E** instead of **C**	54	57:43
6	**F** instead of **C**	89	88:12
7	**G** instead of **C**	36	68:32
8	CH_2Cl_2 instead of THF	51	92:8
9	PhMe instead of THF	68	80:20
10	Boc instead of Bz	52	96:4
11	MeOH instead of NaO*t*-Bu	0	-
12	KO*t*-Bu instead of NaO*t*-Bu	88	93:7
13	LiO*t*-Bu instead of NaO*t*-Bu	82	95:5
14	NaO*s*-amyl instead of NaO*t*-Bu	74	79:21
15	0 °C instead of 23 °C	69	93:3
16	K_2CO_3 instead of Cs_2CO_3	74	94:6
17	2.0 instead of 3.0 equiv. Cs_2CO_3	85	97:3

general catalyst structure

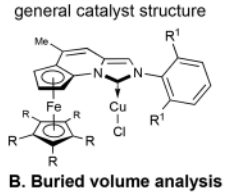

	R	R^1
A	Me	Et
B	Ph	Et
C	Me	OMe
D	Ph	Me
E	Me	*i*-Pr
F	Me	O*i*-Pr
G	Ph	OMe

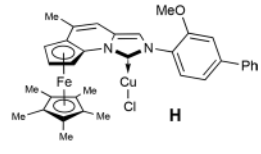

B. Buried volume analysis

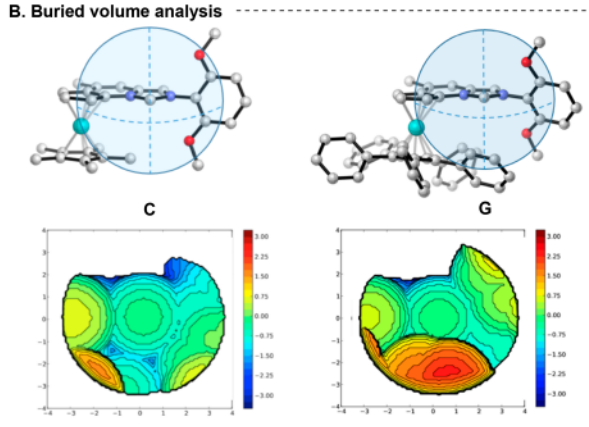

NHC	$\%V_{Bur}$ Total	SW	NW	NE	SE
C	39.5	51.5	33.2	28.0	45.3
G	51.3	68.8	31.9	46.3	58.2

Figure 2. (A) Optimization. (B) Buried volume analysis. [a]See Supporting Information for details. [b]Determined by ^{1}H NMR spectroscopy. [c]Determined by HPLC (chiral stationary phase).

known classes of chiral NHC ligands, we calculated buried volume ($\%V_{Bur}$) on a subset of our NHC-metal complexes. This parameter provides a useful relative assessment of the overall steric encumbrance around a hypothetical metal center for a set of ligands.[17] Our analyses revealed that functionalization of the pendant Cp ring (e.g., pentamethyl-Cp **C** vs pentaphenyl-Cp **G**) had the greatest effect on calculated total buried volume (Figure 2B). Notably, 51.3% of the simulated coordination sphere was occupied for NHC **G**. This value is extremely large for Arduengo-type NHCs, which typically range between 20% and 35%.[17b] Among carbenes, the extremely large $\%V_{Bur}$ of **G** is only approached by Bertrand's CAAC-type NHC ligands ($51.2\%V_{Bur}$)[18] and Glorius's (−)-menthone-derived IBiox NHC ($47.8\%V_{Bur}$).[19] Examining

DOI: 10.1021/jacs.8b05045
J. Am. Chem. Soc. 2018, 140, 10644−10648

Table 1. Substrate Scope[a]

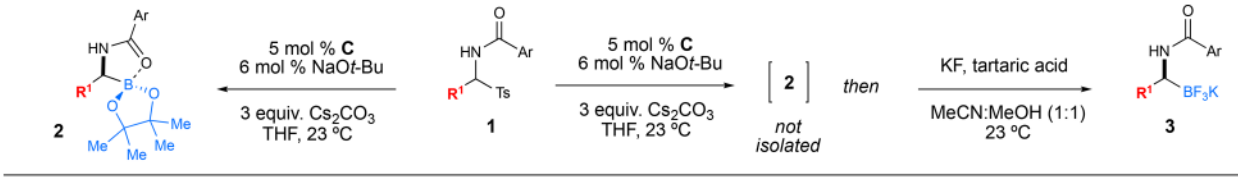

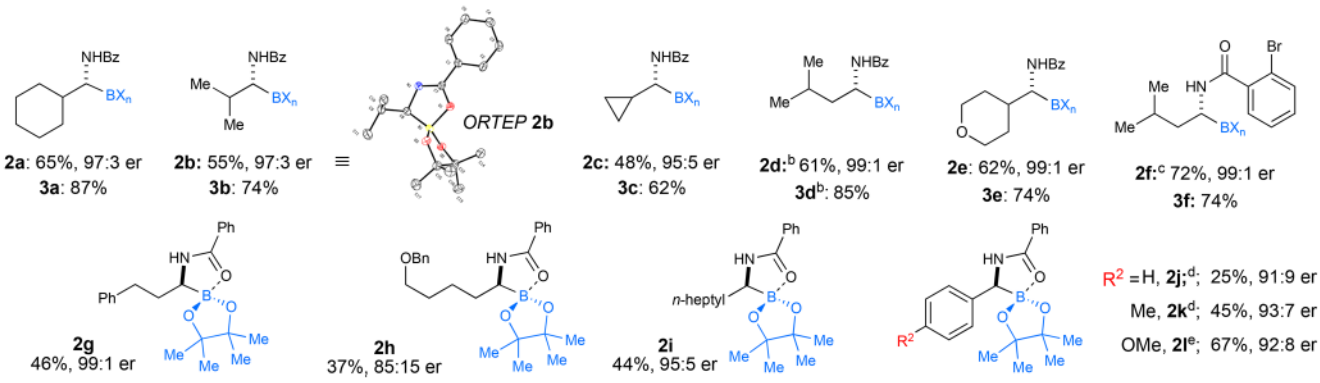

[a]Isolated yields. Enantiomeric ratio was determined by chiral HPLC analysis of the corresponding MIDA boronates. (See SI for details.) [b]Catalyst H was used instead of C. [c]Not isolated (see SI for details). [d]Solvent = MTBE. [e]Solvent = DCM.

other Cp*-derived NHCs revealed the wingtip *N*-aryl group had minimal impact on calculated $\%V_{Bur}$ (39.5%V_{Bur} for C). All complexes examined were characterized by a large occupancy in their "southwest" quadrant (as depicted), where the bulky Cp rings are positioned. The large difference in $\%V_{Bur}$ between C and G demonstrates the potential tunability of these ligands through either simple modulation of the Cp base of the planar NHC scaffold or more complex N-aryl substituents.

We next explored the scope of the asymmetric borylation promoted by catalyst C using our optimized conditions. A variety of primary and secondary α-amido-pinacolatoboronate esters (2) were obtained in excellent enantioselectivity (Table 1). Interestingly, isobutyl-substituted **2d** was obtained with diminished er using catalyst C; however substituting catalyst H furnished **2d** in excellent er (99:1). Product **2f**, possessing a more sterically encumbered *o*-bromobenzoyl protecting group, was also formed with excellent enantioselectivity (99:1). Aryl substrates (2j–l) required alternative solvents to observe good enantioselectivities (MTBE and DCM), albeit with lower isolated yields. Finally, the absolute stereochemistry of **2b** was assigned through X-ray crystallography, revealing catalyst (−)-C produced **2b** in the *S*-configuration.

While we identified conditions that could provide a range of α-amidoboronates with high enantioselectivity, certain products exhibited a large discrepancy between isolated and NMR spectroscopy-based yields. The diminished mass recovery is attributed to SiO_2-catalyzed protodeborylation of the products during conventional chromatographic purification. Potassium trifluoroborate (BF_3K) salts typically exhibit markedly improved stability in relation to their acid and ester analogues, as well as diminished solubility in organic solvents, which often allows their isolation to be conducted via simple precipitation.[20] Thus, we sought means to convert the crude α-amidoboronates (2) to their BF_3K salts (3) in an additional workup step that might circumvent the need for chromatography altogether. Initial attempts at converting some unpurified pinacol esters to their corresponding salts via exposure to an aqueous solution of KHF_2 afforded the desired trifluoroborate in low yields.[21] However, milder conditions developed by Lennox[22] allowed for direct conversion of unpurified enantioenriched α-amido-BPin esters 2 to the corresponding BF_3K salts 3 in a two-step, chromatography-free procedure with considerably improved yields (Table 1, 3a–f).

Cu(I)-mediated borylations are currently understood to proceed through a four-membered transition state involving initial alignment of the Cu–B and X=C bonds.[23] With this foundation, we surmised that in the course of this reaction copper(I) chloride precatalyst C is first converted to active alkoxide I, which can then undergo σ-bond metathesis with B_2Pin_2, to yield copper boryl species II (Figure 3A).

After deprotonation of sulfinyl species 1, the resultant imine (4) can undergo σ-bond metathesis as depicted in transition state III. Protonolysis of amidate IV with *tert*-butanol could yield the product (2), or exchange of IV with an additional equivalent of B_2Pin_2 could afford bis(boronate) 5; then subsequent protonolysis would also lead to product 2.

A model of the observed selectivity in the aldimine borylation is depicted in Figure 3B. Analysis of the crystal structure of catalyst (−)-C, as well as buried volume calculations (see Figure 2), reveals a clearly discernible "open" northwest quadrant. The proposed major transition state (III) depicts an approach of the *E*-aldimine via the top face of the NHC anti to the ferrocene. In this arrangement, the benzoyl group occupies the open quadrant, minimizing steric repulsion with the out-of-plane catalyst *o*,*o*-dimethoxyphenyl ring, possibly participating in stabilizing π-stacking with the ferrocene and its adjacent ring. To fashion a deeper understanding of the composite energetic factors governing catalyst selectivity, we initiated density functional theory (DFT) studies to further elucidate the origins of selectivity in the borylation reaction. The computed major and minor borylation transition states of imine 4 by catalyst C are shown in Figure 4. The major TS leading to the experimentally favored enantiomeric product is 2.3 kcal/mol more stable than the minor TS, in good agreement with experiments ($\Delta G^{\ddagger}$ = 2.1 kcal/mol).

Distortion–interaction analyses of the transition states were performed. The relative imine distortion energies and the

DOI: 10.1021/jacs.8b05045
J. Am. Chem. Soc. 2018, 140, 10644–10648

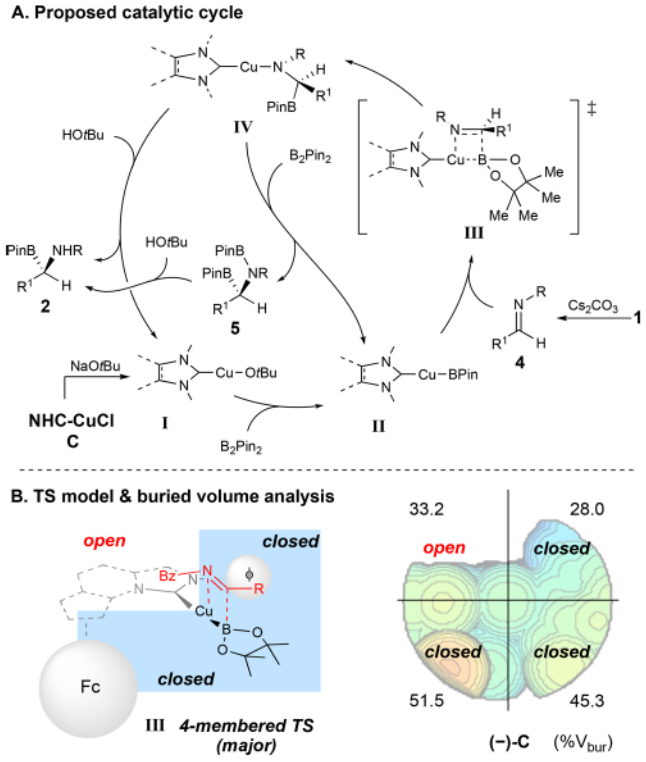

Figure 3. (A) Proposed catalytic cycle. (B) Comparison of major TS model and buried volume analysis of catalyst C (see SI for details).

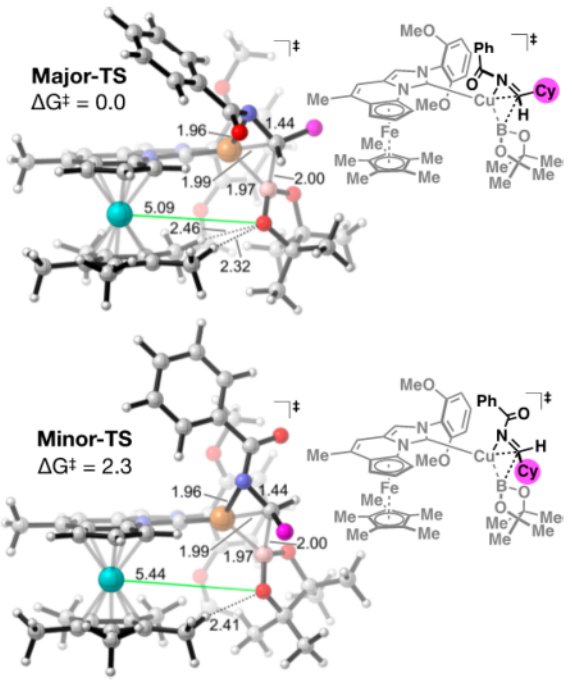

Figure 4. Computed major and minor imine borylation transition structures. Distances in Å and energies in kcal/mol. Cyclohexanes are represented by a single purple sphere.[24]

interaction energies are small and inconsequential (ΔG = 0.7 and −1.1 kcal/mol, respectively). The bulk of the selectivity arises from the differences in distortion energies of the copper-Bpin species (ΔG = 2.6 kcal/mol).

Overlaying these copper-Bpin species found in the two transition states reveals two major differences (see SI): (1) the ferrocene is eclipsed in the minor TS and staggered in the major TS; (2) one of the Bpin oxygens is in closer proximity to the ferrocene in the major TS than the minor TS (O–Fe distance is 5.1 vs 5.4 Å, two C–H···O interactions vs one, respectively). We had originally hypothesized that the eclipsed vs staggered ferrocene conformations may be responsible for the selectivity. To test this hypothesis, we computed the eclipsed and staggered conformations of the copper boryl species II. The staggered was indeed found to be more stable than the eclipsed, but only slightly so (ΔG = 0.5 kcal/mol). This suggested that the Bpin oxygen ferrocene interaction is responsible for the bulk of the difference and therefore the bulk of the stereoselectivity (~2 kcal/mol).[25]

In summary, we have developed the first highly selective catalytic hydroboration of alkyl-substituted aldimines. This approach involves the deployment of new planar-chiral NHC-copper complexes to control the delivery of the boron nucleophile to the *in situ* formed imine. This ligand set provides a distinctive tunable buried volume parameter that could be advantageous in other transition-metal-catalyzed processes. DFT computations provide strong evidence for the stereochemical rationale. The overall synthetic process has been streamlined to be entirely chromatography-free in most cases. This platform can now provide the community with rapid access to a range of α-amidoboronates with medicinally relevant properties that could also serve as versatile building blocks in other metal-catalyzed transformations.

■ ASSOCIATED CONTENT

Supporting Information

The Supporting Information is available free of charge on the ACS Publications website at DOI: 10.1021/jacs.8b05045.

Experimental procedures, spectral data for new compounds, crystallographic data, computed energies, and structures (PDF)
Crystallographic data (CIF)
Crystallographic data (CIF)
Crystallographic data (CIF)
Crystallographic data (CIF)

■ AUTHOR INFORMATION

Corresponding Author

*scheidt@northwestern.edu

ORCID

Paul H.-Y. Cheong: 0000-0001-6705-2962
Karl A. Scheidt: 0000-0003-4856-3569

Notes

The authors declare no competing financial interest.

■ ACKNOWLEDGMENTS

Financial support was generously provided by the NSF (CHE-1665141; CHE-1152010). P.H.Y.C. gratefully acknowledges financial support from the Vicki & Patrick F. Stone family. P.H.Y.C. and A.C.B. thank the National Science Foundation (NSF, CHE-1352663 and CHE-1102637).

■ REFERENCES

(1) (a) Yang, W.; Gao, X.; Wang, B. *Med. Res. Rev.* **2003**, *23*, 346–368. (b) Trippier, P. C.; McGuigan, C. *MedChemComm* **2010**, *1*, 183–198. (c) Ni, N.; Wang, B. Applications of Boronic Acids in Chemical Biology and Medicinal Chemistry. In *Boronic Acids*; Hall, D. G., Ed.; Wiley-VCH Verlag GmbH & Co. KGaA, 2011; pp 591–620.

DOI: 10.1021/jacs.8b05045
J. Am. Chem. Soc. 2018, 140, 10644–10648

(d) Das, B. C.; Thapa, P.; Karki, R.; Schinke, C.; Das, S.; Kambhampati, S.; Banerjee, S. K.; Van Veldhuizen, P.; Verma, A.; Weiss, L. M.; Evans, T. *Future Med. Chem.* **2013**, *5*, 653−676. (e) Leśnikowski, Z. J. *Expert Opin. Drug Discovery* **2016**, *11*, 569−578.
(2) Philipp, M.; Bender, M. L. *Proc. Natl. Acad. Sci. U. S. A.* **1971**, *68*, 478−480.
(3) (a) Valery, M. D.; Abed Al Aziz, Q.; Morris, S. *Mini-Rev. Med. Chem.* **2004**, *4*, 1001−1018. (b) Matteson, D. S. *Med. Res. Rev.* **2008**, *28*, 233−246. (c) Milo, L. J.; Lai, J. H.; Wu, W.; Liu, Y.; Maw, H.; Li, Y.; Jin, Z.; Shu, Y.; Poplawski, S. E.; Wu, Y.; Sanford, D. G.; Sudmeier, J. L.; Bachovchin, W. W. *J. Med. Chem.* **2011**, *54*, 4365−4377. (d) Touchet, S.; Carreaux, F.; Carboni, B.; Bouillon, A.; Boucher, J.-L. *Chem. Soc. Rev.* **2011**, *40*, 3895−3914. (e) Micale, N.; Scarbaci, K.; Troiano, V.; Ettari, R.; Grasso, S.; Zappalà, M. *Med. Res. Rev.* **2014**, *34*, 1001−1069.
(4) Ballatore, C.; Huryn, D. M.; Smith, A. B. *ChemMedChem* **2013**, *8*, 385−395.
(5) (a) Kane, R. C.; Bross, P. F.; Farrell, A. T.; Pazdur, R. *Oncologist* **2003**, *8*, 508−513. (b) Adams, J.; Kauffman, M. *Cancer Invest.* **2004**, *22*, 304−311. (c) Kane, R. C.; Dagher, R.; Farrell, A.; Ko, C.-W.; Sridhara, R.; Justice, R.; Pazdur, R. *Clin. Cancer Res.* **2007**, *13*, 5291−5294.
(6) (a) Andres, P.; Ballano, G.; Calaza, M. I.; Cativiela, C. *Chem. Soc. Rev.* **2016**, *45*, 2291−2307. (b) Clark, T. B. *Asian J. Org. Chem.* **2016**, *5*, 31−42.
(7) (a) Cunningham, C. C. *Expert Opin. Invest. Drugs* **2007**, *16*, 1459−1465. (b) White, J. *Drugs Today* **2011**, *47*, 99−107. (c) Seavey, M. M.; Lu, L. D.; Stump, K. L.; Wallace, N. H.; Ruggeri, B. A. *Int. Immunopharmacol.* **2012**, *12*, 257−270. (d) Hecker, S. J.; Reddy, K. R.; Totrov, M.; Hirst, G. C.; Lomovskaya, O.; Griffith, D. C.; King, P.; Tsivkovski, R.; Sun, D.; Sabet, M.; Tarazi, Z.; Clifton, M. C.; Atkins, K.; Raymond, A.; Potts, K. T.; Abendroth, J.; Boyer, S. H.; Loutit, J. S.; Morgan, E. E.; Durso, S.; Dudley, M. N. *J. Med. Chem.* **2015**, *58*, 3682−3692. (e) Shirley, M. *Drugs* **2016**, *76*, 405−411. (f) Han, L.-Q.; Yuan, X.; Wu, X.-Y.; Li, R.-D.; Xu, B.; Cheng, Q.; Liu, Z.-M.; Zhou, T.-Y.; An, H.-Y.; Wang, X.; Cheng, T.-M.; Ge, Z.-M.; Cui, J.-R.; Li, R.-T. *Eur. J. Med. Chem.* **2017**, *125*, 925−939. (g) Manasanch, E. E.; Orlowski, R. Z. *Nat. Rev. Clin. Oncol.* **2017**, *14*, 417−433.
(8) (a) Sole, C.; Gulyas, H.; Fernandez, E. *Chem. Commun.* **2012**, *48*, 3769−3771. (b) Hong, K.; Morken, J. P. *J. Am. Chem. Soc.* **2013**, *135*, 9252−9254. (c) Zhang, S.-S.; Zhao, Y.-S.; Tian, P.; Lin, G.-Q. *Synlett* **2013**, *24*, 437−442. (d) Wang, D.; Cao, P.; Wang, B.; Jia, T.; Lou, Y.; Wang, M.; Liao, J. *Org. Lett.* **2015**, *17*, 2420−2423. (e) Chen, L.; Zou, X.; Zhao, H.; Xu, S. *Org. Lett.* **2017**, *19*, 3676−3679. (f) López, A.; Clark, T. B.; Parra, A.; Tortosa, M. *Org. Lett.* **2017**, *19*, 6272−6275.
(9) (a) Wityak, J.; Earl, R. A.; Abelman, M. M.; Bethel, Y. B.; Fisher, B. N.; Kauffman, G. S.; Kettner, C. A.; Ma, P.; McMillan, J. L. *J. Org. Chem.* **1995**, *60*, 3717−3722. (b) Matteson, D. S. *J. Org. Chem.* **2013**, *78*, 10009−10023. (c) Ammoscato, V.; Bishop, J. E.; Chiu, F. T.; Geiser, A.; Gomez, J. M.; Hett, R.; Koellner, C.; Kulkarni, V. R.; Lo, Y.; Munk, S. In Google Patents; USPTO, Ed.; Millennium Pharmaceuticals, Inc.: USA, 2016; US20160362449.
(10) (a) Beenen, M. A.; An, C.; Ellman, J. A. *J. Am. Chem. Soc.* **2008**, *130*, 6910−6911. (b) Robak, M. T.; Herbage, M. A.; Ellman, J. A. *Chem. Rev.* **2010**, *110*, 3600−3740. (c) Wen, K.; Chen, J.; Gao, F.; Bhadury, P. S.; Fan, E.; Sun, Z. *Org. Biomol. Chem.* **2013**, *11*, 6350−6356. (d) Wen, K.; Wang, H.; Chen, J.; Zhang, H.; Cui, X.; Wei, C.; Fan, E.; Sun, Z. *J. Org. Chem.* **2013**, *78*, 3405−3409. (e) Buesking, A. W.; Bacauanu, V.; Cai, I.; Ellman, J. A. *J. Org. Chem.* **2014**, *79*, 3671−3677. (f) Chen, J.; Chen, L.-y.; Zheng, Y.; Sun, Z. *RSC Adv.* **2014**, *4*, 21131−21133.
(11) Li, C.; Wang, J.; Barton, L. M.; Yu, S.; Tian, M.; Peters, D. S.; Kumar, M.; Yu, A. W.; Johnson, K. A.; Chatterjee, A. K.; Yan, M.; Baran, P. S. *Science* **2017**, *356*, 356.
(12) (a) Nishikawa, D.; Hirano, K.; Miura, M. *J. Am. Chem. Soc.* **2015**, *137*, 15620−15623. (b) Hu, N.; Zhao, G.; Zhang, Y.; Liu, X.; Li, G.; Tang, W. *J. Am. Chem. Soc.* **2015**, *137*, 6746−6749.
(13) (a) Izquierdo, J.; Orue, A.; Scheidt, K. A. *J. Am. Chem. Soc.* **2013**, *135*, 10634−10637. (b) McCusker, E. O.; Scheidt, K. A. *Angew. Chem., Int. Ed.* **2013**, *52*, 13616−13620. (c) Jang, K. P.; Hutson, G. E.; Johnston, R. C.; McCusker, E. O.; Cheong, P. H.; Scheidt, K. A. *J. Am. Chem. Soc.* **2014**, *136*, 76−79. (d) Liu, K.; Hovey, M. T.; Scheidt, K. A. *Chem. Sci.* **2014**, *5*, 4026−4031. (e) Wang, M. H.; Cohen, D. T.; Schwamb, C. B.; Mishra, R. K.; Scheidt, K. A. *J. Am. Chem. Soc.* **2015**, *137*, 5891−5894. (f) Hovey, M. T.; Cohen, D. T.; Walden, D. M.; Cheong, P. H. Y.; Scheidt, K. A. *Angew. Chem., Int. Ed.* **2017**, *56*, 9864−9867.
(14) Check, C. T.; Jang, K. P.; Schwamb, C. B.; Wong, A. S.; Wang, M. H.; Scheidt, K. A. *Angew. Chem., Int. Ed.* **2015**, *54*, 4264−4268.
(15) (a) Rios, R.; Liang, J.; Lo, M. M. C.; Fu, G. C. *Chem. Commun.* **2000**, 377−378. (b) For a relevant description of the evolution and application of planar chiral ligands in asymmetric catalysis, see: Fu, G. C. *Acc. Chem. Res.* **2006**, *39*, 853−860.
(16) Lee, Y.; Hoveyda, A. H. *J. Am. Chem. Soc.* **2009**, *131*, 3160−3161.
(17) (a) Poater, A.; Cosenza, B.; Correa, A.; Giudice, S.; Ragone, F.; Scarano, V.; Cavallo, L. *Eur. J. Inorg. Chem.* **2009**, *2009*, 1759−1766. (b) Clavier, H.; Nolan, S. P. *Chem. Commun.* **2010**, *46*, 841−861.
(18) Lavallo, V.; Frey, G. D.; Kousar, S.; Donnadieu, B.; Bertrand, G. *Proc. Natl. Acad. Sci. U. S. A.* **2007**, *104*, 13569−13573.
(19) Würtz, S.; Lohre, C.; Fröhlich, R.; Bergander, K.; Glorius, F. *J. Am. Chem. Soc.* **2009**, *131*, 8344−8345.
(20) (a) Molander, G. A.; Wisniewski, S. R. *J. Am. Chem. Soc.* **2012**, *134*, 16856−16868. (b) Molander, G. A. *J. Org. Chem.* **2015**, *80*, 7837−7848. (c) Molloy, J. J.; Watson, A. J. B. B-Protected Boronic Acids: Methodology Development and Strategic Application. In *Boron Reagents in Synthesis*; Coca, A., Ed.; ACS Symposium Series; American Chemical Society: Washington, DC, 2016; pp 379−413.
(21) (a) Vedejs, E.; Chapman, R. W.; Fields, S. C.; Lin, S.; Schrimpf, M. R. *J. Org. Chem.* **1995**, *60*, 3020−3027. (b) Buesking, A. W.; Ellman, J. A. *Chem. Sci.* **2014**, *5*, 1983−1987.
(22) (a) Lennox, A. J. J. Organotrifluoroborate Preparation. In *Organotrifluoroborate Preparation, Coupling and Hydrolysis*; Springer Theses; Springer International Publishing: Cham, 2013; pp 11−36;. (b) Lennox, A. J. J.; Lloyd-Jones, G. C. *Angew. Chem., Int. Ed.* **2012**, *51*, 9385−9388.
(23) (a) Zhao, H.; Dang, L.; Marder, T. B.; Lin, Z. *J. Am. Chem. Soc.* **2008**, *130*, 5586−5594. (b) Chong, C. C.; Kinjo, R. *ACS Catal.* **2015**, *5*, 3238−3259. (c) Kubota, K.; Jin, M.; Ito, H. *Organometallics* **2016**, *35*, 1376−1383.
(24) Structures were optimized using B3LYP-D3BJ/6-31G(d)//SMD(THF) level of theory. Final energy refinements were computed using M06/6-31G(d)//SMD(THF). See Supporting Information for full list of citations.
(25) Similar interactions have been proposed to be important for stereoselectivity in planar-chiral organocatalytic reactions involving the ferrocene based organocatalyst PPY*, see: Pattawong, O.; Mustard, T. J. L.; Johnston, R. C.; Cheong, P. H.-Y. *Angew. Chem., Int. Ed.* **2013**, *52*, 1420−1423.

DOI: 10.1021/jacs.8b05045
J. Am. Chem. Soc. 2018, 140, 10644−10648